


PAPER

[View Article Online](#)
[View Journal](#) | [View Issue](#)Cite this: *Dalton Trans.*, 2025, **54**,
3619

Facile preparation, mechanochromic luminescence and excitation wavelength-dependent emission of tetra(1*H*-benzo[d]imidazol-2-yl)ethene Zn(II) complexes and their applications†

Su-Jia Liu,^{†a} Yong-Sheng Shi,^{†a,b} Rui-Ying Wang,^a Tong Xiao,^a Zhong-Gang Xia,^a
Rui Wang^a and Xiang-Jun Zheng^{ib}  [✉]

Nowadays, benzimidazole and its derivatives are widely assembled into multifunctional materials with various properties such as mechanochromism, photochromism, thermochromism and electrochromism. Herein, two novel zinc(II) coordination compounds, [Zn₂(L²)Br₄]·2H₂O (**1**) and [Zn₂(L²)Cl₄]·2H₂O (**2**) (L² = tetra(1*H*-benzo[d]imidazol-2-yl)ethene), have been constructed *via* one-pot facile synthesis from bis(1*H*-benzo[d]imidazol-2-yl)methane (L¹) and zinc(II) salts. The ligand L² with a C=C double bond was *in situ* formed by C–C coupling of two sp³-C atoms of L¹ in solvothermal synthesis, which provides a new strategy to generate the conjugation system conveniently. Impressively, complex **1** shows distinct fluorescence and phosphorescence dual emission due to the heavy atom effect of bromide ions. Complexes **1** and **2** exhibit high-contrast mechanochromic luminescence properties due to the transformation from a crystalline state to an amorphous state. In addition, they also exhibited excitation wavelength-dependent luminescence in crystalline states and DMF systems. As the excitation wavelength increased, their luminescence color in DMF solution changed significantly from blue to yellow. Theoretical calculations show that the complexes have multiple emission centers due to the locally excited nature and intramolecular charge transfer. Due to their excellent excitation wavelength-dependent luminescence properties, PMMA films based on complexes **1** and **2** were prepared and could be applied in anti-counterfeiting and UV protection.

Received 11th December 2024,
Accepted 20th January 2025

DOI: 10.1039/d4dt03434a

rsc.li/dalton

Introduction

Multi-stimuli responsive materials, whose original properties can be changed differently due to some external stimulus such as force,^{1–6} heat,^{7–11} pH^{12–15} and light,^{16–20} now have a wide range of applications in information storage and encryption, sensors, and other fields.^{21–29} Compared to common organic materials, metal–organic complexes have high designability and adjustable luminescence properties. By selecting suitable ligands and metal ions, it is possible to develop new simple synthetic methods to construct multi-stimuli responsive com-

plexes with excellent properties. As a star molecule for aggregation-induced emission luminogens, tetraphenylethene (TPE) has been paid a lot of attention.^{30–34} If the phenyl group is changed to the benzimidazole group, more coordination sites and hydrogen bonding sites would be introduced besides the original character of TPE. More importantly, the introduction of hetero nitrogen atoms would be beneficial for phosphorescence. Bis(1*H*-benzo[d]imidazol-2-yl)methane (L¹), as a unique nitrogen-containing heterocyclic compound, possesses rotatable aromatic rings and may form weak intermolecular interactions (such as hydrogen-bond interaction and $\pi\cdots\pi$ stacking interaction). In addition, the methylene group in the L¹ structure is highly active and can turn into a carbonyl compound by an *in situ* reaction in the presence of metal ions.³⁵ This process was proved to proceed through a ligand oxygenation mechanism. This character provides a possibility to create complexes based on ligands with novel structures and diverse stimulus-response properties. Zhang's group successfully synthesized a tetra(1*H*-benzo[d]imidazol-2-yl)ethene Cu(I) complex through a freezing-melting process for the removal of oxygen and a solvothermal method.³⁶

^aBeijing Key Laboratory of Energy Conversion and Storage Materials, College of Chemistry, Beijing Normal University, Beijing 100875, P. R. China.E-mail: xjzheng@bnu.edu.cn^bCollege of Chemistry and Chemical Engineering, Jiangxi Science and Technology Normal University, Nanchang 330013, P.R. China†Electronic supplementary information (ESI) available. CCDC 2373214 and 2373223. For ESI and crystallographic data in CIF or other electronic format see DOI: <https://doi.org/10.1039/d4dt03434a>

‡These authors contributed equally to this work.

Inspired by the above research, in this work, we have designed and synthesized two binuclear complexes $[\text{Zn}_2(\text{L}^2)\text{Br}_4]\cdot 2\text{H}_2\text{O}$ (**1**) and $[\text{Zn}_2(\text{L}^2)\text{Cl}_4]\cdot 2\text{H}_2\text{O}$ (**2**) through simple *in situ* self-assembly of zinc bromide/chloride and L^1 without the freezing–melting process. The ligand L^2 is an analogue of TPE.

Both complexes **1** and **2** exhibit fluorescence and phosphorescence dual emission behaviours, and complex **1** shows obvious phosphorescence emissions due to the presence of the heavy-atom effect. After grinding, complexes **1** and **2** show high-contrast mechanochromic luminescence properties, which can be attributed to a transition from a crystalline state to an amorphous state. Furthermore, complexes **1** and **2** show excitation wavelength-dependent emission in their crystalline states and DMF solution systems, which can be ascribed to the structure of multiple emission centers. Their major emissions in DMF solution exhibit an obvious red-shift with the increase of the excitation wavelength, leading to a transformation of their emission colour from blue to yellow. Owing to the outstanding excitation wavelength-dependent emission properties of complexes **1** and **2**, their PMMA films were successfully made and applied in anti-counterfeiting and UV protection.

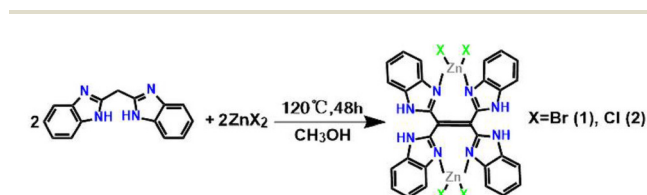
Experimental section

Synthesis of L^1

L^1 was synthesized based on a literature procedure.³⁷ L^1 : ^1H NMR (600 MHz, $\text{DMSO}-d_6$) δ (ppm): 12.38 (s, 2H), 7.51 (s, 2H), 7.43 (s, 2H), 7.11 (s, 4H), 2.46 (s, 2H) (Fig. S1†).

Synthesis of $[\text{Zn}_2(\text{L}^2)\text{Br}_4]\cdot 2\text{H}_2\text{O}$ (**1**)

Complex **1** was synthesized using an *in situ* synthesis method as shown in Scheme 1. L^1 (24 mg, 0.1 mmol), $\text{ZnBr}_2\cdot 2\text{H}_2\text{O}$ (78.4 mg, 0.3 mmol) and CH_3OH (4 mL) were mixed and stirred at room temperature for 5 min. Then the resulting solution was placed in a 25 mL Teflon-lined stainless-steel reactor at 120 °C for 48 h. The product was collected, washed in CH_3OH , and dried in air at room temperature. Yellow bulk crystals of **1** (CCDC number 2373214) were collected. Yield: 40.86% (based on L^1). IR (KBr pellet, cm^{-1}): 3480 m, 3263 m, 1631 s, 1591 s, 1426 s, 1352 w, 1210 w, 1070 m, 940 w, 741 s (Fig. S2a†). Anal. calcd for $\text{C}_{30}\text{H}_{24}\text{N}_8\text{O}_2\text{Zn}_2\text{Br}_4$ (FW: 978.96): C, 36.77%; H, 2.45%; N, 11.44%; found: C, 36.75%; H, 2.49%; N, 11.40%.



Scheme 1 Synthetic routes of complexes **1** and **2**.

Synthesis of $[\text{Zn}_2(\text{L}^2)\text{Cl}_4]\cdot 2\text{H}_2\text{O}$ (**2**)

The synthesis method of complex **2** is the same as that of **1**, and **2** can be obtained by replacing $\text{ZnBr}_2\cdot 2\text{H}_2\text{O}$ with $\text{ZnCl}_2\cdot 2\text{H}_2\text{O}$ in system **1**. Yellow bulk crystals **2** (CCDC number 2373223) were collected. Yield: 45.07% (based on L^1). IR (KBr pellet, cm^{-1}): 3463 m, 3243 m, 1613 s, 1426 s, 1361 s, 1222 m, 1064 m, 779 s, 744 s (Fig. S2b†). Anal. calcd for $\text{C}_{30}\text{H}_{24}\text{N}_8\text{O}_2\text{Zn}_2\text{Cl}_4$ (FW: 801.12): C, 44.94%; H, 3.00%; N, 13.98%; found: C, 44.89%; H, 3.07%; N, 13.95%.

Results and discussion

Characterization of complexes **1** and **2**

In the presence of zinc(II) ions, two L^1 ligands react through carbon–carbon coupling to form the L^2 ligand *via* a one-pot *in situ* reaction. It is speculated that this process involves a ligand oxygenation mechanism and carbonyl olefination *via* the McMurry coupling reaction.^{38,39}

Single-crystal X-ray diffraction (XRD) studies indicate that complex **1** crystallizes in the triclinic crystal system with the space group $P\bar{1}$ (Table S1†). The asymmetric unit of complex **1** contains one Zn^{2+} ion, half of the L^2 ligand, two Br^- ions and a free H_2O molecule, which forms a binuclear $[\text{Zn}_2(\text{L}^2)\text{Br}_4]\cdot 2\text{H}_2\text{O}$ structure (Fig. 1a). After carbon–carbon coupling, the double bond length is 1.347 Å. The Zn–N bond length is in the range of 2.039–2.049 Å. The bond angles around Zn centers range from 89.42° to 116.25° (Table S2†). The dihedral angle between the two benzimidazole rings, Cg1 (C5–C6–N2–C7–N1) and Cg2 (C10–C11–N3–C9–N4), is 85.0°. There are hydrogen bond interactions between N3–H3...Br2 and N2–H2...O1 with distances of 2.67 Å and 1.94 Å, respectively. There are also some other weak interactions that make complex **1** more stable, such as $\pi\cdots\pi$ stacking between the benzene ring Cg3 (C10–C11–C12–C13–C14–C15) and the benzene ring Cg3 on adjacent layers and C–H... π interactions between C13–H13 and the imidazole ring Cg1 (Table S3†). So, the 0D structure is extended to a 2D chain structure due to these intermolecular hydrogen bonds and weak interactions (Fig. 1b).

Single-crystal X-ray diffraction (XRD) studies indicate that the crystal structure of complex **2** is similar to that of **1** (Fig. S3†), but the dihedral angles and the distances of intermolecular and intramolecular interactions are slightly

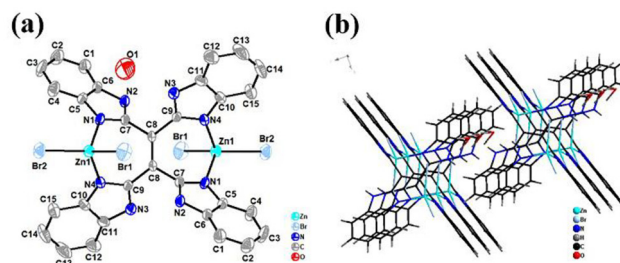


Fig. 1 (a) Molecular structure of complex **1**; (b) the stacking form of complex **1**.

different (Table S3†). The carbon–carbon double bond length is 1.353 Å. The Zn–N bond length is in the range of 2.029–2.040 Å. The bond angles around Zn centers range from 89.82° to 118.90° (Table S2†).

Thermogravimetric analyses (TGA) were also conducted to investigate the thermochromic behaviour of complexes **1** and **2** (Fig. S4†). The first weight loss of 3.7% and 4.6% starts from 25 to 100 °C corresponding to the removal of water molecules (cal. 3.7% and 4.5%). The complexes began to decompose at about 400 °C, demonstrating that they exhibit good thermal stability.

Luminescence properties

The luminescence spectrum of complex **1** was recorded. When excited at 428 nm, complex **1** showed two emission peaks at 463 and 640 nm, respectively (Fig. 2a). Then the lifetime of these two emission peaks was determined (Fig. S5†). The decay curve showed that the emission peak at 463 nm had a lifetime of 0.43 ns, which belonged to fluorescence emission. The emission peak at 640 nm had a lifetime of 331 μs, indicative of the nature of phosphorescence emission. This indicates that complex **1** has dual emission behaviour of fluorescence and phosphorescence.

The emission spectrum of complex **2** (Fig. 2b) shows a single peak. However, it can be observed that its emission peak has a tailing phenomenon at longer wavelengths. A peak-splitting operation was carried out with two peaks at 515 and 570 nm obtained (Fig. S6a†). The emission peak at 570 nm has a lifetime of 6.55 μs, indicating that complex **2** also possesses phosphorescent emission behaviour (Fig. S6b†). However, the heavy-atom effect of Cl is not as obvious as that of Br, and the phosphorescent emission of complex **2** is weak and covered by the fluorescence emission peak, so it does not show an obvious dual emission like complex **1**.

Mechanochromic luminescence properties

As mentioned above, both Zn(II) complexes have rotatable benzimidazole rings in their structures and display distorted spatial conformations, which makes them a type of promising stimulus-responsive material. The luminescence behaviour of complexes **1** and **2** in different states was investigated to assess whether they possess mechanochromic luminescence properties. As shown in Fig. 3a, when complex **1** was excited at

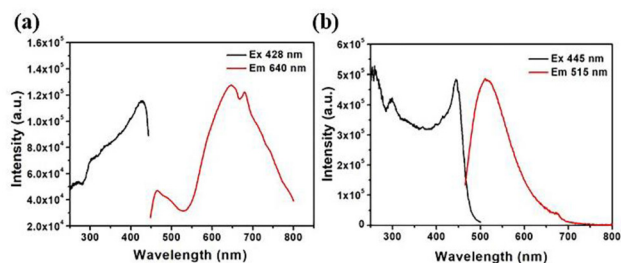


Fig. 2 Excitation and emission spectra of complexes **1** (a) and **2** (b).

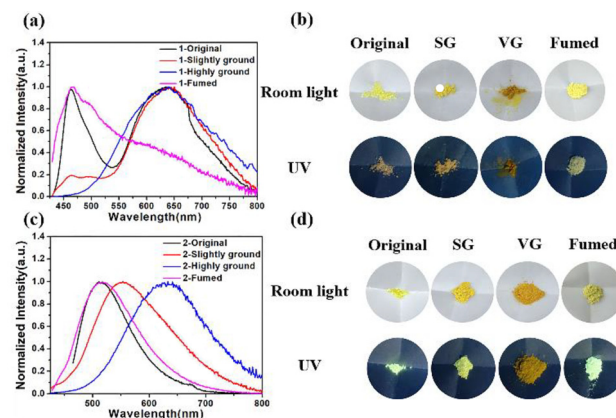


Fig. 3 Emission spectra of complexes **1** (a) and **2** (c) in different states; (b) photographs of complexes **1** (b) and **2** (d) in different states (original, slightly ground, vigorously ground, and fumed) under sunlight and 365 nm UV illumination.

365 nm, its original crystal showed comparable intensity of dual emissions at 463 and 640 nm, emitting light orange luminescence. Upon slight mechanical grinding, the relative intensity of these two peaks was altered, with a relative decrease at 463 nm and a relative increase at 640 nm. After thorough grinding, only the emission peak at 640 nm was left and the luminescence colour appeared as orange-red. The emission peak at 463 nm can be recovered after fuming the fully ground sample with methanol vapour. The alternating process between complete grinding and fumigation can be repeated for multiple cycles (Fig. S7a†). In addition, the colour before and after grinding under room light changed from light yellow to orange, which could be clearly observed, and it was also confirmed by the solid-state UV-visible spectrum (Fig. S8a†). All the above phenomena indicate that complex **1** has mechanochromic luminescence properties. Complex **2** also has similar properties, as shown in Fig. 3c. The original crystal of complex **2** showed green luminescence emission at 515 nm. After slight grinding, the emission peak showed a red-shift to 554 nm. Finally, after vigorous grinding, the fully ground sample showed an orange luminescence emission at 630 nm. When fuming with methanol vapour, the emission peak can recover to 515 nm. This alternating process can also be repeated for many cycles (Fig. S7b†). The colour of complex **2** before and after grinding under room light also changed significantly (Fig. 3d). In conclusion, the two Zn(II) complexes are promising materials with excellent mechanochromic luminescence properties.

To further understand the mechanism of mechanochromic luminescence properties, PXRD experiments were performed. The original samples of complex **1** and complex **2** showed strong and sharp diffraction peaks, indicating their crystalline nature (Fig. 4). After slight grinding, the diffraction peaks became broad, yet some sharp peaks still remained, indicating that the ordered arrangement changed a little. After complete grinding, an amorphous state was observed, suggesting that

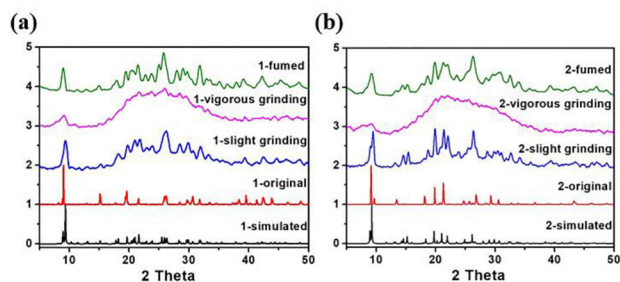


Fig. 4 (a) PXRD patterns of complex **1** before and after grinding and fuming and (b) PXRD patterns of complex **2** before and after grinding and fuming.

the change of luminescence emission was caused by the transformation from a crystalline to an amorphous state. After being fumed with methanol vapour, some characteristic diffraction peaks were recovered, indicating the recovery of the lattice.

As mentioned above, complexes **1** and **2** exhibited high contrast mechanochromic luminescence properties, which can be applied in force test paper. The sample of complex **2** was dispersed on filter paper to make the test paper. As shown in Fig. 5, when writing “BNU” on the test paper with a glass stick, a fuzzy orange handwriting can be seen under sunlight, and a clear orange emission “BNU” can be seen under UV light. Then exposure to methanol vapour could erase the letter under sunlight and UV light.

Excitation wavelength-dependent emission properties

Considering that complexes **1** and **2** exhibit dual emission with a wide range of excitation between 250 and 450 nm (Fig. 2), we further investigate their luminescence with their crystals and DMF solutions in detail. As shown in Fig. 6a, complex **1** in the crystalline state exhibits a typical excitation-wavelength-dependent emission. With the excitation wavelength ranging from 300 to 420 nm, the luminescence spectra show an obvious intensity change of bimodal peaks centered at 463 and 640 nm. Generally, it can be observed that the emission intensity of these two bands gradually increases with the increase of the excitation wavelength, but the change of emis-

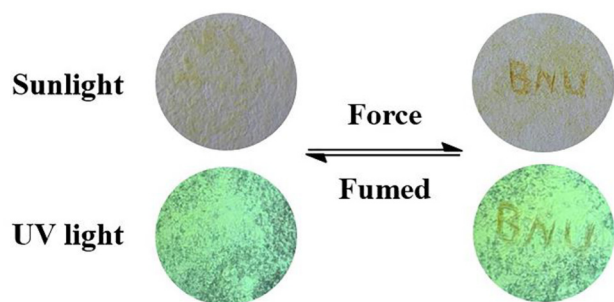


Fig. 5 Photographs of the test paper of complex **2** taken under sunlight and 365 nm UV light after writing and fuming with methanol.

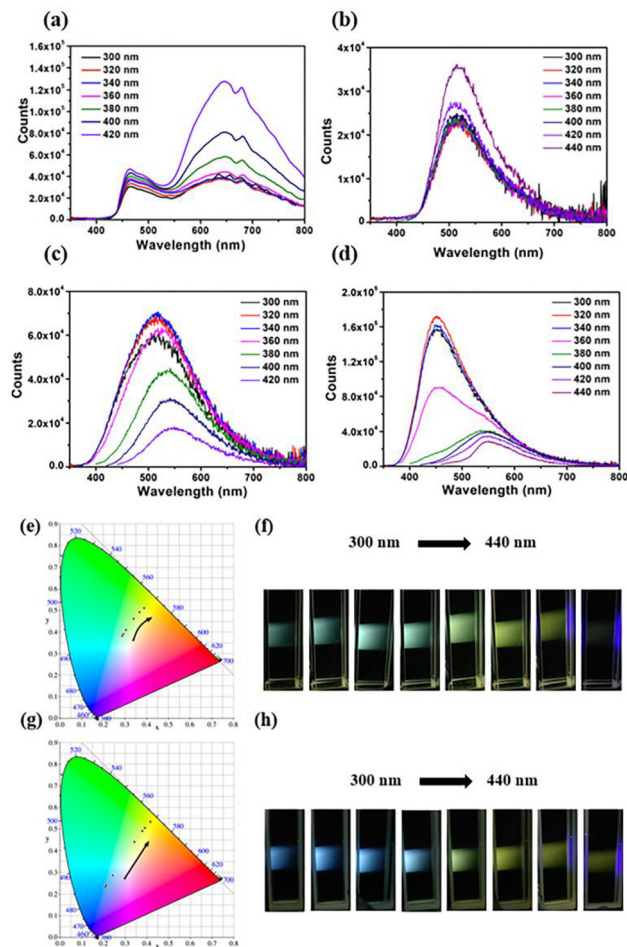


Fig. 6 Emission spectra of complexes **1** (a) and **2** (b) in the crystal state excited by different excitation wavelengths; emission spectra of complexes **1** (c) and **2** (d) in DMF solution excited by different excitation wavelengths; the CIE chromaticity diagram revealing the dynamic luminescence colour change of complexes **1** (e) and **2** (g) in DMF solution excited by different wavelengths; the dynamic luminescence colour change of complexes **1** (f) and **2** (h) in DMF solution excited by light from 300 nm to 440 nm.

sion intensity centered at 640 nm is much larger than that at 463 nm. According to the 1931 Commission Internationale de l'Eclairage (CIE) coordinate diagram, its colour changed from light orange to orange-red, with the change of the initial coordinate ($x = 0.3962$, $y = 0.3592$) to ($x = 0.4716$, $y = 0.3726$) (Fig. S9a†). The change in luminescence of complex **2** in the crystalline state is not obvious, because its heavy-atom effect is not as significant as that of complex **1** (Fig. 6b).

Then complexes **1** and **2** in DMF solutions with a concentration of 0.005 g dL^{-1} were prepared, and their emission spectra excited by different excitation wavelengths were recorded (Fig. 6c and d). It can be seen that the major emission wavelength of complex **1** in DMF solution obviously changes due to the increase of the excitation wavelength. It gradually changed from 514 to 547 nm, and the colour changed from cyan to yellow (Fig. 6f). The CIE coordinate

diagram showed the luminescence changes from the initial coordinate ($x = 0.2869$, $y = 0.381$, cyan) to ($x = 0.3877$, $y = 0.5106$, yellow) (Fig. 6e). Similarly, the major emission wavelength of complex 2 also changed from 451 to 550 nm, accompanied by the colour changing from blue to cyan, which finally became yellow (Fig. 6h). The CIE diagram also clearly verified the change of this process from the initial coordinates ($x = 0.2134$, $y = 0.2392$, blue) to ($x = 0.4159$, $y = 0.5340$, yellow) (Fig. 6g).

In order to understand the mechanism of excitation wavelength-dependent emission properties, the structures of complexes 1 and 2 were optimized and calculated using the Gaussian 09 program (opt freq wb97xd/sdd) (Fig. 7). It can be seen that the highest occupied molecular orbital (HOMO) of complexes 1 and 2 is distributed on the ligand moiety, particularly on the C=C group, and the lowest unoccupied molecular orbital (LUMO) is mainly located on ZnX_2 ($\text{X} = \text{Cl}, \text{Br}$) and the central C=C group. The HOMO and LUMO are not separated. This implies that the complexes have a locally excited nature with a large contribution of intramolecular charge transfer, generating multiple emission centers, which contributes to the excitation wavelength-dependent emission.

Application in films

In recent years, luminescence anti-counterfeiting has attracted increasing attention due to its excellent optical properties.^{40–43} Considering the excitation wavelength-dependent emission performance of complexes 1 and 2, their potential application in anticounterfeiting was explored. A type of PMMA film device was made, hoping to greatly extend the application of this material. First, a mixture of PMMA (5 g), complex 1/complex 2 (5 mg) and DMF (100 mL) was stirred until they were completely dissolved. Then the solution was placed on a glass plate and heated in an oven until the solvent evaporated

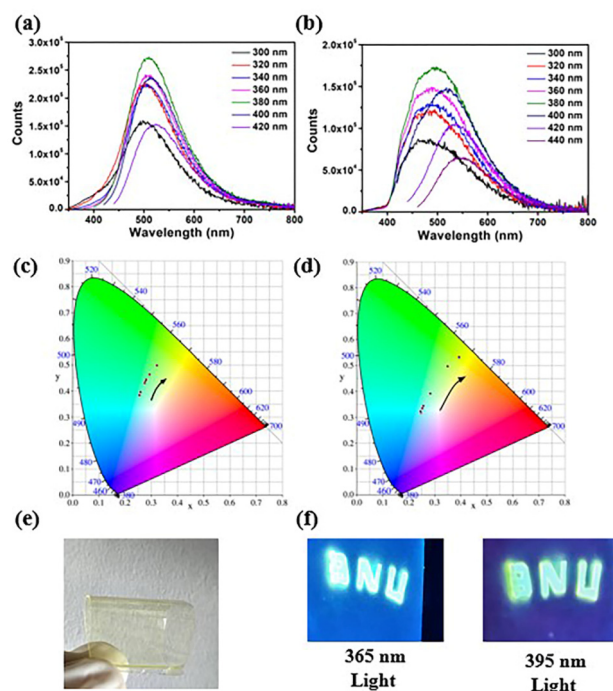


Fig. 8 Emission spectra of complexes 1 (a) and 2 (b) in the PMMA film excited by different excitation wavelengths; the CIE chromaticity diagram revealing the dynamic luminescence colour change of complexes 1 (c) and 2 (d) in the PMMA film excited by different wavelengths of light; (e) flexibility of the PMMA film; (f) complex 2 in the PMMA film exhibiting different colours excited by 365 and 395 nm for anti-counterfeiting applications.

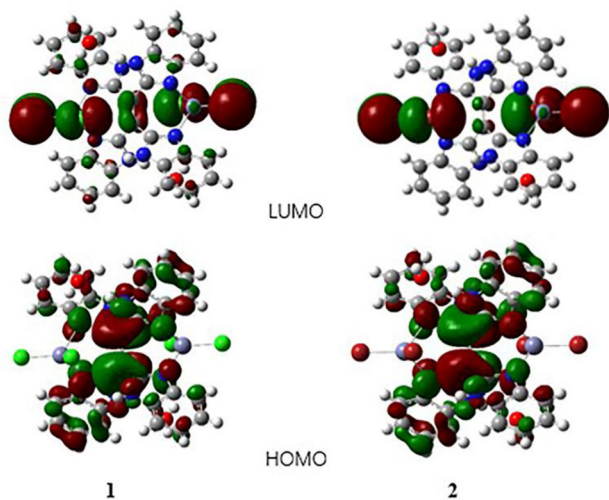


Fig. 7 The optimized molecular configurations and HOMO and LUMO of complexes 1 and 2.

completely to result in films. These films could be folded and bent with good flexibility (Fig. 8e). As expected, the particular properties of the designed film are similar to those in DMF solutions (Fig. 8a and b).

The unique excitation wavelength-dependent emission properties make complexes 1 and 2 in PMMA films an excellent system for anti-counterfeiting. After excitation with different wavelengths of light, these films show different luminescence. This process is clearly verified in the CIE diagram (Fig. 8c and d). The coordinates of complex 1 change from ($x = 0.2548$, $y = 0.3845$, blue) to ($x = 0.3210$, $y = 0.4986$, yellow green), and those of complex 2 also change from ($x = 0.2466$, $y = 0.3168$, blue) to ($x = 0.3928$, $y = 0.5314$, yellow). Taking the PMMA film of complex 2 as an example, we cut it into a pattern with the “BNU” shape. As shown in Fig. 8f, its luminescence colour appears blue under 365 nm excitation and yellow-green under 395 nm excitation, which shows a dual information anti-counterfeiting process.

In addition, the PMMA films of complexes 1 and 2 have unique absorption in the range of 250–450 nm (Fig. S10†). So, these films can also be used as UV protection devices, such as sunglasses. In summary, excellent excitation wavelength-dependent luminescence and UV absorption characteristics make this PMMA film a type of ideal anti-counterfeiting and UV protection device.

Conclusions

In summary, we have successfully synthesized two multi-stimuli responsive zinc(II) complexes (**1** and **2**) based on a TPE analogue. We first found that bis(1*H*-benzo[*d*]imidazol-2-yl) methane can undergo a carbon–carbon coupling process by *in situ* synthesis in the presence of zinc(II) ions, which greatly simplifies the operation steps compared with previous literature. Both complexes have fluorescence and phosphorescence dual emission. Complex **2** has a better phosphorescence behaviour due to the heavy-atom effect of bromide ions. They exhibit high contrast mechanochromic luminescence. PXRD indicates that the grinding and fuming processes of complexes **1** and **2** correspond to the transformation between crystalline and amorphous states. The luminescence of complexes **1** and **2** was dependent on the excitation wavelength both in the crystalline state and in DMF solution. Theoretical calculations imply that the complexes have multiple emission centers, which contribute to the excitation wavelength-dependent emission. PMMA films of complexes **1** and **2** also show excitation wavelength-dependent emission similar to that in DMF solution and have been proven to be excellent anti-counterfeiting devices. Their strong absorption in the UV range endows them with potential applications in UV protection. This work provides new insights into the syntheses of complexes with multi-stimuli responses.

Author contributions

Xiang-Jun Zheng: conceptualization, formal analysis, funding acquisition, writing – review, and supervision. Su-Jia Liu: validation, investigation, formal analysis, and writing – original draft. Yong-Sheng Shi: conceptualization, methodology, and software. Rui-Ying Wang: formal analysis and investigation. Tong Xiao: investigation. Zhong-Gang Xia: validation. Rui Wang: validation.

Data availability

Additional structural figures, ¹H NMR, IR, fluorescence decay curves, fluorescence emission, UV-Vis, TGA curves, crystal data and structure refinement, and selected bond distances and angles.

CCDC 2373214 and 2373223 contain the supplementary crystallographic data for **1** and **2**.

Conflicts of interest

There are no conflicts to declare.

Acknowledgements

The authors acknowledge the financial support from the National Natural Science Foundation of China (21671022).

References

- 1 D. Sun, Y. Wu, X. Han and S. Liu, *Nat. Commun.*, 2023, **14**, 4190.
- 2 L. Li, X. Yin, Y.-X. Zhao, L.-Y. Shi, K.-K. Yang and Y.-Z. Wang, *J. Mater. Chem. A*, 2024, **12**, 18117–18126.
- 3 Y. Pan, H. Zhang, P. Xu, Y. Tian, C. Wang, S. Xiang, R. Boulatov and W. Weng, *Angew. Chem., Int. Ed.*, 2020, **59**, 21980–21985.
- 4 S. Zhang, C. Sun, J. Zhang, S. Qin, J. Liu, Y. Ren, L. Zhang, W. Hu, H. Yang and D. Yang, *Adv. Funct. Mater.*, 2023, **33**, 2305364.
- 5 Y. Yang, X. Yang, X. Fang, K. Z. Wang and D. Yan, *Adv. Sci.*, 2018, **5**, 1801187.
- 6 M. Raisch, W. Maftuhin, M. Walter and M. Sommer, *Nat. Commun.*, 2021, **12**, 4243.
- 7 I. Jurewicz, A. A. K. King, R. Shanker, M. J. Large, R. J. Smith, R. Maspero, S. P. Ogilvie, J. Scheerder, J. Han, C. Backes, J. M. Razal, M. Florescu, J. L. Keddie, J. N. Coleman and A. B. Dalton, *Adv. Funct. Mater.*, 2020, **30**, 2002473.
- 8 B. Deng, Y. Zhu, X. Wang, J. Zhu, M. Liu, M. Liu, Y. He, C. Zhu, C. Zhang and H. Meng, *Adv. Mater.*, 2023, **35**, 2302685.
- 9 T. Xu, Y. Han, Y. Ni and C. Chi, *Angew. Chem., Int. Ed.*, 2024, **64**, e202414533.
- 10 J. C. Liu, W. Q. Liao, P. F. Li, Y. Y. Tang, X. G. Chen, X. J. Song, H. Y. Zhang, Y. Zhang, Y. M. You and R. G. Xiong, *Angew. Chem., Int. Ed.*, 2020, **59**, 3495–3499.
- 11 S.-Z. Sheng, J.-L. Wang, B. Zhao, Z. He, X.-F. Feng, Q.-G. Shang, C. Chen, G. Pei, J. Zhou, J.-W. Liu and S.-H. Yu, *Nat. Commun.*, 2023, **14**, 3231.
- 12 B.-B. Ma, H. Zhang, Y. Wang, Y.-X. Peng, W. Huang, M.-K. Wang and Y. Shen, *J. Mater. Chem. C*, 2015, **3**, 7748–7755.
- 13 N. A. Vodolazkaya, N. O. McHedlov-Petrosyan, G. Heckenkemper and C. Reichardt, *J. Mol. Liq.*, 2003, **107**, 221–234.
- 14 X.-F. Wang, C.-Y. Xu, R.-L. Lin, W.-Q. Sun, M.-F. Ye, L.-X. Xu and J.-X. Liu, *J. Mater. Chem. C*, 2024, **12**, 2764–2771.
- 15 F. Heidari, H. Roghani-Mamaqani, H. Mardani and S. Talebi, *Eur. Polym. J.*, 2024, **210**, 112942.
- 16 H. Kuroiwa, Y. Inagaki, K. Mutoh and J. Abe, *Adv. Mater.*, 2018, **31**, 1805661.
- 17 C.-C. Ko and V. W.-W. Yam, *Acc. Chem. Res.*, 2017, **51**, 149–159.
- 18 J.-X. Wang, C. Li and H. Tian, *Coord. Chem. Rev.*, 2021, **427**, 213579.

- 19 X.-T. Li, M.-J. Li, Y.-L. Tian, S.-L. Han, L. Cai, H.-C. Ma, Y.-Q. Zhao, G.-J. Chen and Y.-B. Dong, *Nat. Commun.*, 2024, **15**, 8484.
- 20 N. M. W. Wu, M. Ng and V. W. W. Yam, *Angew. Chem., Int. Ed.*, 2018, **58**, 3027–3031.
- 21 X. Bi, Y. Shi, T. Peng, S. Yue, F. Wang, L. Zheng and Q. E. Cao, *Adv. Funct. Mater.*, 2021, **31**, 2101312.
- 22 T. Zheng, G. G. Li, F. Zhou, R. Wu, J. J. Zhu and H. Wang, *Adv. Mater.*, 2016, **28**, 8218–8226.
- 23 Z. Guo, Y. Bian, L. Zhang, J. Zhang, C. Sun, D. Cui, W. Lv, C. Zheng, W. Huang and R. Chen, *Adv. Mater.*, 2024, **36**, 2409361.
- 24 K. Endo, H. Ube and M. Shionoya, *J. Am. Chem. Soc.*, 2019, **142**, 407–416.
- 25 Y. Jiang, J. Ma, Z. Ran, H. Zhong, D. Zhang and N. Hadjichristidis, *Angew. Chem., Int. Ed.*, 2022, **61**, e202208516.
- 26 X. Fu, L. Hosta-Rigau, R. Chandrawati and J. Cui, *Chem.*, 2018, **4**, 2084–2107.
- 27 J. Sheng, J. Perego, S. Bracco, W. Czepa, W. Danowski, S. Krause, P. Sozzani, A. Ciesielski, A. Comotti and B. L. Feringa, *Adv. Mater.*, 2023, **36**, 2305783.
- 28 L. Jia, S. Zeng, H. Ding, A. T. Smith, A. M. LaChance, M. M. Farooqui, D. Gao, J. Ma and L. Sun, *Adv. Funct. Mater.*, 2021, **31**, 2104427.
- 29 W. Dai, X. Niu, X. Wu, Y. Ren, Y. Zhang, G. Li, H. Su, Y. Lei, J. Xiao, J. Shi, B. Tong, Z. Cai and Y. Dong, *Angew. Chem., Int. Ed.*, 2022, **61**, e202200236.
- 30 M. Hu, F.-Y. Ye, C. Du, W. Wang, T.-T. Zhou, M.-L. Gao, M. Liu and Y.-S. Zheng, *ACS Nano*, 2021, **15**, 16673–16682.
- 31 X. Nie, W. Huang, D. Zhou, T. Wang, X. Wang, B. Chen, X. Zhang and G. Zhang, *Aggregate*, 2022, **3**, e165.
- 32 G. Huang, Y. Jiang, S. Yang, B. S. Li and B. Z. Tang, *Adv. Funct. Mater.*, 2019, **29**, 1900516.
- 33 J. Liu, J. Sheng, L. Shao, Q. Zheng, W. Li, X. Chen, L. Mao and M. Wang, *Angew. Chem., Int. Ed.*, 2021, **60**, 26740–26746.
- 34 M. Hu, F. Y. Ye, C. Du, W. Wang, W. Yu, M. Liu and Y. S. Zheng, *Angew. Chem., Int. Ed.*, 2021, **61**, e202115216.
- 35 H.-C. Yao, M.-M. Li, G.-S. Yang, Z.-J. Li and Y. Zhu, *Inorg. Chim. Acta*, 2007, **360**, 3959–3964.
- 36 K.-K. Feng, J.-S. Wu, Y.-P. Li, Y.-A. Tan and Z. Xin, *Inorg. Chem. Commun.*, 2023, **158**, 111710.
- 37 F. D. S. Miranda, F. G. Menezes, J. Vicente, A. J. Bortoluzzi, C. Zucco, A. Neves and N. S. Gonçalves, *J. Mol. Struct.*, 2009, **938**, 1–9.
- 38 A. Schultz, S. Diele, S. Laschat and M. Nimtz, *Adv. Funct. Mater.*, 2001, **11**, 441–446.
- 39 F. Zhang, Y. Zhang, L. Sun, C. Wei, H. Zhang, L. Wu, X. Ge and T. Xu, *Angew. Chem., Int. Ed.*, 2022, **62**, e202215017.
- 40 B.-M. Liu, Y. Lin, Y. Liu, B. Lou, C.-G. Ma, H. Zhang and J. Wang, *Light: Sci. Appl.*, 2024, **13**, 286.
- 41 J. Koo, M. Kim, J. Hyeong, D. Yu, S. Kim, J. Jang, M. Oh, Y. Wi, H. Ko and K. U. Jeong, *Adv. Opt. Mater.*, 2023, **11**, 2300844.
- 42 K. Wang, J. Shi, W. Lai, Q. He, J. Xu, Z. Ni, X. Liu, X. Pi and D. Yang, *Nat. Commun.*, 2024, **15**, 3203.
- 43 G. Liu, X. Wu, F. Xiong, J. Yang, Y. Liu, J. Liu, Z. Li, Z. Qin, S. Deng and B.-R. Yang, *Light: Sci. Appl.*, 2024, **13**, 198.